

Single-shot implementation of dispersion-scan for the characterization of ultrashort laser pulses

D. Fabris,¹ W. Holgado,² F. Silva,^{3,4} T. Witting,¹ J. W. G. Tisch,^{1,5} and H. Crespo³

¹Blackett Laboratory, Imperial College, London SW7 2AZ, UK

²Grupo de Investigación en Óptica Extrema (GIOE), Universidad de Salamanca, E-37008 Salamanca, Spain

³IFIMUP-IN e Departamento de Física e Astronomia, Faculdade de Ciências, Universidade do Porto, 4169-007 Porto, Portugal

⁴fsilvaporugal@gmail.com

⁵john.tisch@imperial.ac.uk

Abstract: We demonstrate a single-shot ultrafast diagnostic, based on the dispersion-scan (d-scan) technique. In this implementation, rather than translating wedges to vary the dispersion as in scanning d-scan, the pulse to be measured experiences a spatially varying amount of dispersion in a prism. The resulting beam is then imaged into a second-harmonic generation crystal and an imaging spectrometer is used to measure the two-dimensional trace, which is analyzed using the d-scan retrieval algorithm. We compare the single-shot implementation with the scanning d-scan for the measurement of sub-3.5-fs pulses from a hollow core fiber pulse compressor. We show that the retrieval algorithm used to extract amplitude and phase of the pulse provides comparable results, proving the validity of the new single-shot implementation in the near single-cycle regime.

©2015 Optical Society of America

OCIS codes: (320.7100) Ultrafast measurements; (320.7110) Ultrafast nonlinear optics; (320.7160) Ultrafast technology; (320.5520) Pulse compression.

References and links

1. I. A. Walmsley and C. Dorrer, "Characterization of ultrashort electromagnetic pulses," *Adv. Opt. Photonics* **1**(2), 308–437 (2009).
2. J.-H. Chung and A. Weiner, "Ambiguity of ultrashort pulse shapes retrieved from the intensity autocorrelation and the power spectrum," *IEEE J. Sel. Top. Quantum Electron.* **7**(4), 656–666 (2001).
3. F. Krausz and M. Ivanov, "Attosecond physics," *Rev. Mod. Phys.* **81**(1), 163–234 (2009).
4. E. Esarey, C. B. Schroeder, and W. P. Leemans, "Physics of laser-driven plasma-based electron accelerators," *Rev. Mod. Phys.* **81**(3), 1229–1285 (2009).
5. D. J. Kane and R. Trebino, "Characterization of arbitrary femtosecond pulses using frequency-resolved optical gating," *IEEE J. Quantum Electron.* **29**(2), 571–579 (1993).
6. C. Iaconis and I. A. Walmsley, "Spectral phase interferometry for direct electric-field reconstruction of ultrashort optical pulses," *Opt. Lett.* **23**(10), 792–794 (1998).
7. R. Trebino, K. W. DeLong, D. N. Fittinghoff, J. N. Sweetser, M. A. Krumbugel, B. A. Richman, and D. J. Kane, "Measuring ultrashort laser pulses in the time-frequency domain using frequency-resolved optical gating," *Rev. Sci. Instrum.* **68**(9), 3277–3295 (1997).
8. E. M. Kosik, A. S. Radunsky, I. A. Walmsley, and C. Dorrer, "Interferometric technique for measuring broadband ultrashort pulses at the sampling limit," *Opt. Lett.* **30**(3), 326–328 (2005).
9. J. R. Birge, R. Ell, and F. X. Kartner, "Two-dimensional spectral shearing interferometry for few-cycle pulse characterization," *Opt. Lett.* **31**(13), 2063–2065 (2006).
10. A. Baltuska, M. S. Pshenichnikov, and D. A. Wiersma, "Second-harmonic generation frequency-resolved optical gating in the single-cycle regime," *IEEE J. Quantum Electron.* **35**(4), 459–478 (1999).
11. J. R. Birge, H. M. Crespo, and F. X. Kartner, "Theory and design of two-dimensional spectral shearing interferometry for few-cycle pulse measurement," *J. Opt. Soc. Am. B* **27**(6), 1165–1173 (2010).
12. T. Witting, F. Frank, W. A. Okell, C. A. Arrell, J. P. Marangos, and J. W. G. Tisch, "Sub-4-fs laser pulse characterization by spatially resolved spectral shearing interferometry and attosecond streaking," *J. Phys. At. Mol. Opt. Phys.* **45**(7), 074014 (2012).
13. P. O'Shea, M. Kimmel, X. Gu, and R. Trebino, "Highly simplified device for ultrashort-pulse measurement," *Opt. Lett.* **26**(12), 932–934 (2001).

14. A. S. Radunsky, E. M. Williams, I. A. Walmsley, P. Wasylczyk, W. Wasilewski, A. B. U'Ren, and M. E. Anderson, "Simplified spectral phase interferometry for direct electric-field reconstruction by using a thick nonlinear crystal," *Opt. Lett.* **31**(7), 1008–1010 (2006).
15. M. Miranda, T. Fordell, C. Arnold, A. L'Huillier, and H. Crespo, "Simultaneous compression and characterization of ultrashort laser pulses using chirped mirrors and glass wedges," *Opt. Express* **20**(1), 688–697 (2012).
16. M. Miranda, C. L. Arnold, T. Fordell, F. Silva, B. Alonso, R. Weigand, A. L'Huillier, and H. Crespo, "Characterization of broadband few-cycle laser pulses with the d-scan technique," *Opt. Express* **20**(17), 18732–18743 (2012).
17. F. Silva, M. Miranda, B. Alonso, J. Rauschenberger, V. Pervak, and H. Crespo, "Simultaneous compression, characterization and phase stabilization of GW-level 1.4 cycle VIS-NIR femtosecond pulses using a single dispersion-scan setup," *Opt. Express* **22**(9), 10181–10191 (2014).
18. F. Böhle, M. Kretschmar, A. Jullien, M. Kovacs, M. Miranda, R. Romero, H. Crespo, U. Morgner, P. Simon, R. Lopez-Martens, and T. Nagy, "Compression of CEP-stable multi-mJ laser pulses down to 4 fs in long hollow fibers," *Laser Phys. Lett.* **11**(9), 095401 (2014).
19. B. Alonso, M. Miranda, F. Silva, V. Pervak, J. Rauschenberger, J. San Román, Í. J. Sola, and H. Crespo, "Characterization of sub-two-cycle pulses from a hollow-core fiber compressor in the spatiotemporal and spatio-spectral domains," *Appl. Phys. B* **112**(1), 105–114 (2013).
20. F. Silva, M. Miranda, S. Teichmann, M. Baudish, M. Massicotte, F. Koppens, J. Biegert, and H. Crespo, "Near to mid-IR ultra-broadband third harmonic generation in multilayer graphene: few-cycle pulse measurement using THG dispersion-scan," in *Proceedings of CLEO: 2013, OSA Technical Digest (online)* (OSA, 2013), paper CW1H.5.
21. M. Hoffmann, T. Nagy, T. Willemsen, M. Jupé, D. Ristau, and U. Morgner, "Pulse characterization by THG d-scan in absorbing nonlinear media," *Opt. Express* **22**(5), 5234–5240 (2014).
22. F. Siva, M. Miranda, and H. Crespo, "Measuring few-cycle laser pulses: A comparative study between dispersion-scan and FROG," *Lasers and Electro-Optics Europe (CLEO EUROPE/IQEC), 2013 and International Quantum Electronics Conference*, 12–16 May 2013, doi: 10.1109/CLEOE-IQEC.2013.6801095.
23. M. Miranda, P. Rudawski, C. Guo, F. Silva, C. Arnold, T. Binhammer, H. Crespo, and A. L'Huillier, "Ultrashort laser pulse characterization from dispersion scans: a comparison with SPIDER," in *Proceedings of CLEO: 2013, OSA Technical Digest (online)* (Optical Society of America, 2013), paper JTh2A.31.
24. D. R. Austin, T. Witting, and I. A. Walmsley, "Broadband astigmatism-free Czerny-Turner imaging spectrometer using spherical mirrors," *Appl. Opt.* **48**(19), 3846–3853 (2009).
25. P. Hello and C. N. Man, "Design of a low-loss off-axis beam expander," *Appl. Opt.* **35**(15), 2534–2536 (1996).

1. Introduction

In the ultrafast domain, optical pulse characterization poses a significant challenge [1]. Basic autocorrelation techniques only give limited and incomplete information about the pulse duration [2], especially with the advent of shorter and more complex to measure pulses that possess structured spectra and non-trivial spectral phase profiles. Moreover, such ultra-broadband pulses are exploited in experiments and applications dependent on the details of the pulse waveform and carrier-envelope phase, such as attoscience [3] and high-field physics [4]. Hence, there is growing demand for accurate and reliable pulse diagnostics capable of dealing with ultra-broadband pulses with durations down to the single-cycle or even sub-cycle regime.

Different approaches have been developed to characterize broadband pulses by retrieving amplitude and/or phase information. The two most common measurement techniques are frequency resolved optical gating (FROG) [5] and spectral phase interferometry for direct electric field reconstruction (SPIDER) [6], with all their respective variants – see, e.g [1, 7–12]. These are extremely versatile and powerful techniques that normally involve operations such as temporal overlap of short pulses, beam splitting and recombination. Important simplified implementations of FROG [13] and SPIDER [14] have been demonstrated, but additional challenges arise when measuring few-cycle and octave-spanning pulses, due to the need to preserve their ultra-broad bandwidths in all pulse manipulation steps, and because of the required large phase matching bandwidths [10–12]. The dispersion-scan (d-scan) technique [15, 16] enables the simultaneous measurement and compression of femtosecond laser pulses and has been originally proposed as a way to simplify such steps, making both the setup and the data acquisition process as simple as possible while still providing robust and precise pulse retrieval. In fact it involves only the measurement of a spectrum multiple

times as a function of dispersion applied to the pulse. The d-scan technique however is not as studied as more established techniques like FROG and SPIDER, which warrants further development. For this reason several experiments have already been performed with d-scan on various pulses [15–18]. The combination of the d-scan and STARFISH techniques has enabled the spatiotemporal and spatio-spectral characterization of sub-two-cycle laser pulses, both collimated and on focus [19]. Third-harmonic variants of d-scan have been successfully demonstrated based on multilayer graphene [20] and on thin films with variable bandgaps [21]. Comparative studies between d-scan and FROG [22] and d-scan and SPIDER [23] performed using few-cycle pulses revealed very good agreement between techniques.

So far, single-shot d-scan is yet to be demonstrated and this is the main focus of the present work. Single-shot capability is of great interest, not only for low repetition rate lasers, where the nature of the experiments is inherently based on the shot-to-shot characterization of the system, but also for higher repetition rate systems where the reproducibility of the pulses may be achieved via feedback loops or where data-tagging techniques are employed.

2. Concept and experiment

In the scanning d-scan [15], the second-harmonic of the pulse under investigation is generated in a nonlinear crystal and the resulting spectrum is measured as a function of the introduced dispersion using a 1-D spectrometer. The complete measurement is built up over a large number of shots as the dispersion is scanned, usually by varying the amount of glass insertion using a motorized wedge pair. Pulse characterization through d-scan is based on the fact that when a pulse undergoes a nonlinear conversion process, such as second-harmonic generation (SHG), the resulting spectral intensity has a well-defined dependence on the input spectral phase. By measuring the spectrum of the nonlinear signal for different input phases (glass insertions) around the point of maximum compression, a two-dimensional trace is obtained that enables the full retrieval of the spectral phase of the pulses via an iterative algorithm. Additionally, d-scan has an inline and robust setup, without the need of beam splitting, beam recombination or interferometric precision.

For a single-shot implementation of d-scan we aim to acquire the two-dimensional trace required by the d-scan algorithm without the need for moving parts. The concept of our single-shot implementation is depicted in Fig. 1. A spatially variable amount of dispersion is imparted on the beam profile using a glass prism. The resulting SHG signal is re-imaged into a thin SHG crystal using reflective optics. The resulting SHG signal is then re-imaged onto a broadband imaging spectrometer with minimized aberrations [24], which provides a spatially resolved second-harmonic spectrum, $S(x, \lambda)$ [7], where each spectral slice at a given x corresponds to a second-harmonic spectrum obtained with a different amount of dispersion. Unlike scanning d-scan, but like most other pulse diagnostics, this single-shot implementation does not provide simultaneous pulse compression for applications/experiments.

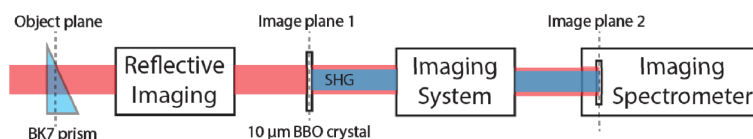


Fig. 1. Schematic of the single-shot d-scan concept and implementation.

The experimental setup is shown in Fig. 2. The laser system used in the experiment is the CPA system (Femtolasers GmbH) and Ar-filled hollow core fiber (HCF) pulse compressor described in [17], which includes a water cell for third-order dispersion compensation. The output of this system, which is capable of producing pulses in the single-cycle regime with energies up to 200 μJ , could be directed both to a scanning d-scan setup and to the single-shot implementation with a flip mirror, in order to achieve a direct comparison of the two diagnostics. The scanning d-scan setup is based on that in [17], but employs a 10 μm thick

BBO crystal (instead of 5 μm) for SHG, and a broadband wire grid polarizer (Thorlabs, Inc.) to separate the second-harmonic signal from the fundamental (instead of the previous scheme comprising a spatial mask, Brewster-angled reflection and slit). The thicker BBO crystal is important for achieving a high signal-to-noise ratio in the single-shot system, which uses the same nonlinear crystal as the scanning d-scan. Although the 10 μm thick crystal has a narrower phase matching bandwidth compared to the 5 μm crystal, this does not prevent the d-scan algorithm from fully retrieving the pulses. This stems from the intrinsic robustness of d-scan with respect to bandwidth limitations in the measured second-harmonic signal, an important property presented in [15] and further demonstrated with few-cycle pulses [16, 17].

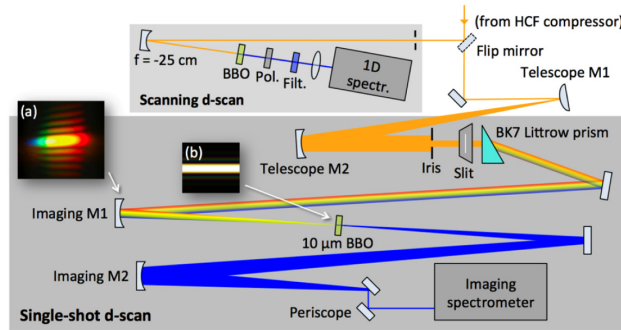


Fig. 2. Optical setup, comprising the scanning d-scan setup (top) and the new single-shot d-scan implementation (bottom) – see text for more details.

The beam directed to the single-shot d-scan was expanded with a telescope (magnification factor $M = 3$), with two spherical mirrors positioned such that astigmatism was avoided [25]. This expansion is necessary to obtain a spatially uniform beam profile, by selecting the central portion of the expanded beam in order to minimize the intrinsic spatio-temporal coupling of this type of source [19]. An iris was used to select a beam diameter of approximately 11 mm. The beam was then transmitted through a 400 μm horizontal slit and directed to a N-BK7 Littrow prism with 30-60-90° angles (Edmund Optics Ltd.) to introduce a spatially varying dispersion along the beam. The size of the beam and the apex angle of the prism allowed for a glass insertion difference between the two extrema of the beam of 5 mm (corresponding to a group-delay dispersion range of approximately 220 fs^2), which is sufficient to have a confined and retrievable d-scan trace for the near-single-cycle pulse under investigation [17]. For pulses longer than a few cycles, a more dispersive prism material and/or a larger beam size can in principle be employed. The output plane of the prism was re-imaged by a spherical mirror ($f = 45$ cm) onto a BBO crystal (10 μm thick, 1 cm square, cut for type-I SHG at 795 nm), with a magnification factor $M = -0.33$. Light transmitted through the slit and prism becomes spatially chirped at the plane of the focusing mirror due to angular dispersion in the prism. This is shown in Fig. 2(a), which also displays wavelength-dependent diffraction from the slit. Nevertheless, the image produced by the focusing mirror at the plane of the thin BBO crystal is free from such effects (Fig. 2(b)). Ray tracing analysis showed that this system effectively provides aberration free imaging. The focusing also ensures sufficient intensity at the BBO crystal (estimated at 65 ± 10 GW/cm^2 for maximum pulse compression) to obtain a detectable second-harmonic signal and allow us to collect the full spatial information, with a linear correspondence between spatial position on the prism surface and spatial position on the BBO. This was achieved by re-imaging the SHG from the BBO crystal onto the entrance slit of the imaging spectrometer by a second spherical mirror ($f = 50$ cm). In this way the spatially dependent dispersion was mapped to the spatial axis of the imaging spectrometer. The calibration of the dispersion axis in the case of the scanning d-scan is straightforward. Once the wedge pair is positioned perpendicularly to the incoming beam, the stage step size can be directly converted to the corresponding glass insertion amount by

simple trigonometry. In the case of the single-shot d-scan the dispersion axis calibration was performed in a similar way. A pair of motorized wedges was positioned in the beam and different amounts of glass were inserted. The effect on the trace measured with the imaging spectrometer was a linear position shift in the spatial axis direction, as expected [15], thus further confirming the expected linear correspondence of different amounts of dispersion to different positions. From this information the pixel-to-insertion calibration can be performed.

3. Results and analysis

Two data sets are shown. The first is the scanning d-scan trace, performed by recording different SHG spectra as a function of wedge insertion. The second is the trace measured in single-shot mode with the imaging spectrometer. The two data sets were taken consecutively by removing the flip mirror shown in Fig. 2. Due to the reduced sensitivity of the camera in the ultraviolet (UV) region, we opted for integration times of 200 ms in order to increase the signal-to-noise ratio (up to 33 dB) for our proof of concept measurement. Nevertheless, the diagnostic is intrinsically scan free and potentially capable of measuring a single pulse.

The measured and retrieved traces are shown in Fig. 3. The single-shot measurement could not cover the same spectral region as the scanning one, especially for the shorter wavelengths, due to the poor spectral response of the CCD camera in the UV.

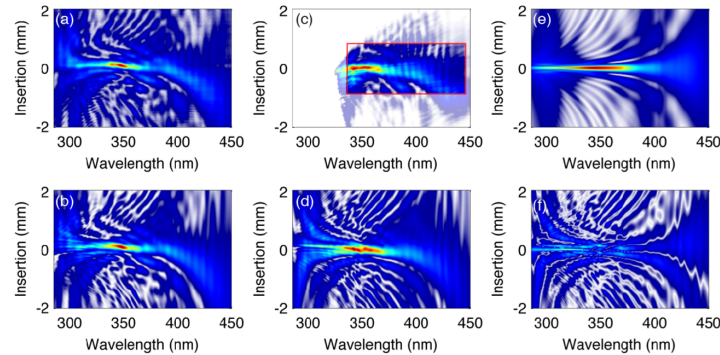


Fig. 3. Experimental d-scan traces measured with the scanning (a) and single-shot (c) setups. The retrievals are shown in (b) and (d), respectively. The simulated trace for a transform-limited (TL) pulse is given in (e); (f) is the difference between TL (e) and single-shot (d) cases.

We limited the portion of the single-shot traces used in the retrieval to the area within the red rectangle in Fig. 3(c), containing approximately 80% of the measured energy in the signal, so as to exclude regions with poor signal-to-noise ratio. Again, this is not too detrimental for retrieval, which can cope with partial traces, as shown in [17] and evidenced here by the similarity between the retrieved traces for both setups in Figs. 3(b) and 3(d) – note the trace features outside the main pulse that are faithfully retrieved by the algorithm from the single-shot trace, even though they are not part of the measurement and clearly differ from those in the trace simulated for the transform-limited case, as shown in Figs. 3(e) and 3(f). Since the windows over which the signal was considered were different for each method, it is not meaningful to directly compare the corresponding retrieval errors (as defined in [15]). Nonetheless, the error over the full represented window is 2% for the scanning measurement and 9% for the single-shot case – the difference mainly due to the missing signal in the latter.

The pulses retrieved from the traces are shown in Fig. 4. The input spectrum necessary for the retrieval algorithm is shown in Fig. 4(a) (Fourier limit of 2.8 fs), while in Fig. 4(b) the two retrieved spectral phases are presented, showing an overall good agreement over the main portion of the spectrum, from 530 to 990 nm. The blue curves correspond to 16 independent retrievals performed from the scanning trace under different initial conditions (random spectral phases), while the black curve is the spectral phase retrieved from the single-shot

measurement (average of 16 independent retrievals); the grey area is the corresponding standard deviation. In both methods, we see that the higher-order phase is less well retrieved than the average/global phase, as evidenced by the opposing rapid phase oscillations over the central portion of the spectrum, from 700 to 800 nm, and the higher rms errors associated with them. The temporal results are shown in Fig. 4(c). The relatively small insertion and wavelength ranges of the single-shot trace compared to the scanning trace increase the difference in the pre- and post-pulse structure around the main pulse, but the results from both methods are nevertheless comparable. The agreement between the two main parts of the temporal profiles is very good, with the pulse duration measured with the scanning and the single-shot setups resulting in 3.2 ± 0.1 fs and 3.3 ± 0.1 fs, respectively.

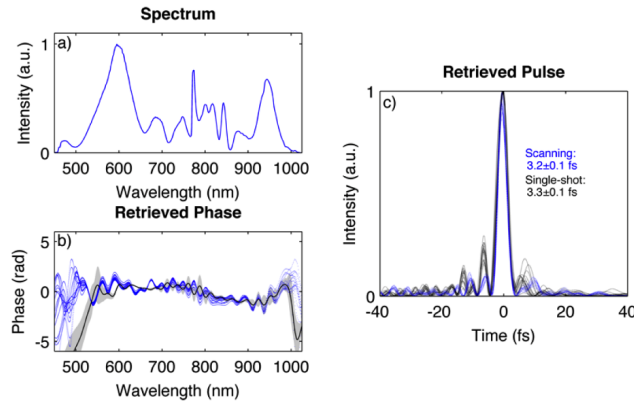


Fig. 4. Pulses retrieved from the two d-scan setups: (a) measured spectrum; (b) comparison of the retrieved spectral phase for the scanning (blue curves, 16 independent retrievals) and the single-shot (black curve) setups. The grey area is the error on the single-shot retrieval (based on 16 independent retrievals). The corresponding pulses are shown in (c) (same color code).

4. Conclusions

We have presented a single-shot implementation of the d-scan pulse characterization technique. A spatially dependent amount of dispersion was applied to the beam with a prism, and then the spatially resolved second-harmonic spectrum was recorded with an imaging spectrometer. Such a setup is able to measure, in a single-shot, the d-scan trace of the pulse. We measured a near-single-cycle pulse from an Ar-filled hollow core fiber pulse compressor and compared the results of the wedge-scanning implementation with data from the single-shot implementation. The agreement between the global spectral phase retrieved in the two configurations is very good, resulting in 3.2 ± 0.1 fs (FWHM) near single-cycle pulses in the scanning measurement and 3.3 ± 0.1 fs in the single-shot measurement, proving the validity of the new single-shot implementation for near single-cycle pulse durations. The single-shot implementation makes the benefits of the d-scan technique available to laboratories with lower repetition rate laser systems or to those using feedback or data-tagging techniques where diagnostics that average over multiple shots are unsuitable.

Acknowledgments

We gratefully acknowledge financial support from the European Science Foundation through the SILMI programme (Short Visit Grant 5585), the UK Engineering and Physical Sciences Research Council (grants EP/F034601/1 and EP/I032517/1) and FCT - Fundação para a Ciência e Tecnologia (grant PTDC/FIS/122511/2010), co-funded by COMPETE and FEDER. H. Crespo and F. Silva acknowledge support from FCT grants SFRH/BSAB/105974/2015 and SFRH/BD/69913/2010, respectively. W. Holgado acknowledges support from Junta de Castilla y León (grant SA116U13, UIC16) and MINECO (FIS2013-44174-P).